Journal of Applied Mechanics and Technical Physics, Vol. 49, No. 3, pp. 491–499, 2008

THERMOELASTOPLASTIC DEFORMATION OF A THICK-WALLED CYLINDER WITH A RADIAL CRACK

I. M. Lavit and Nguyen Viet Trung

UDC 539.375

The thermoelastoplastic fracture mechanics problem of a thick-walled cylinder subjected to internal pressure and a nonuniform temperature field is solved by the method of elastic solutions combined with the finite-element method. The correctness of the solution is provided by using the Barenblatt crack model, in which the stress and strain fields are regular. The elastoplastic problem of a cracked cylinder subjected to internal pressure and a nonuniform temperature field are solved. The calculation results are compared with available data.

Key words: *thick-walled cylinder, crack, fracture, thermoplasticity, cohesive force, cohesive zone.*

Introduction. In strength analysis, structural members used in power and chemical engineering can be treated as thick-walled cylinders subjected to internal pressure and a nonuniform temperature field. Under quasistatic loading, fracture of a cylinder is a results of radial crack propagation from the inner surface. The length of the segment of steady crack growth is comparable to the thickness of the cylinder; therefore, the strength of the cylinder should be analyzed using the fracture mechanics concepts. In addition, it is necessary to take into account the possibility of plastic deformation.

The computational scheme of the problem is given in Fig. 1. A cylinder of inner radius R_1 and outer radius R_2 is in a plane strain state. It is assumed that the material of the cylinder is homogeneous, isotropic, and perfectly plastic and that its strain is small. In elastic deformation, the behavior of the material obeys Hooke's law, and in plastic deformation, it obeys the Prandtl–Reuss relations and the Mises yield condition. The yield point σ_Y depends on temperature. The cylinder is weakened by a radial crack of length a. The interior of the cylinder and the crack cavity are acted upon by pressure p. The cylinder is heated nonuniformly. By virtue of the quasistatic formulation of the problem, the temperature field can be considered axisymmetric.

The problem of elastic deformation of a cracked cylinder was first solved by Bowie and Freese [1] using the Kolosov–Muskhelishvili method with a conformal mapping of a circular ring onto the cross section of the cracked cylinder combined with a collocation method. Only the action of external pressure was considered. Shannon [2] solved the problem of the action of internal pressure using a finite-element method. In this case, unlike in the case considered in [1], pressure was also applied to the crack faces. Andrasis and Parker [3–5] improved the method proposed in [1] and solved a linear fracture mechanics problem for a cylinder containing a varied number of identical cracks equidistant from each and subjected to external and internal pressures, and also in the presence of a self-balanced field of residual stresses. Pu and Hussain [6] solved the same problem using the finite-element method. The elastoplastic deformation of cracked cylinders have also been studied. Sumpter [7] solved an elastoplastic problem for a cylinder subjected to internal pressure using the finite-element method, and Tan and Lee [8] found the same solution using the boundary-element method. Cheissoux [9] studied a thermoelastoplastic problem for a cracked cylinder using the finite-element method and Zhigun [10] examined an elastoplastic problem in the presence of residual stresses after autofregatting.

The solutions of the problems given in [7–10] have a common drawback. As is known, elastic and elastoplastic states differ in the nature of singularities of the stress and strain fields at the crack tip [11]. Because elastoplastic

Tula State University, Tula 300600; IgorLavit@yandex.ru. Translated from Prikladnaya Mekhanika i Tekhnicheskaya Fizika, Vol. 49, No. 3, pp. 173–183, May–June, 2008. Original article submitted June 18, 2007.

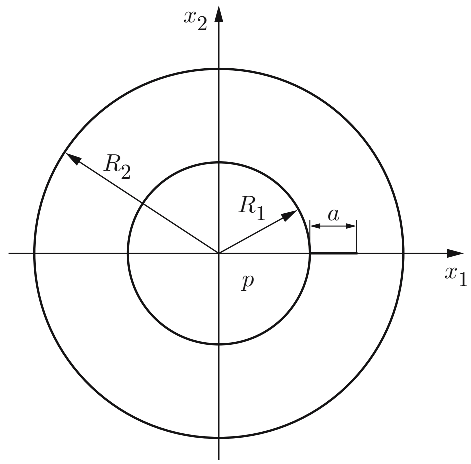

Fig. 1. Computational scheme.

problems are solved using successive approximations, this singularity cannot be taken into account correctly (unlike in solutions of elastic problems) using special elements to satisfy the adopted law of singularity. The standard method for refining numerical solutions — the use of a finer mesh in the zone of maximum stresses — is suitable in this case if the approximation of the singular field near the singular point can be further improved through the use of piecewise analytical functions. In practice, this possibility is established empirically, by comparing numerical elastic solutions obtained on different meshes with a reference solution found by any special method of linear fracture mechanics. It is clear that this approach differs from the method of constructing convergent elastoplastic solutions. It might be expected that, in solving the same problem and having good agreement between the elastic solution and the reference, one would obtain greatly different elastoplastic solutions [12]. Therefore, in solving a thermoelastoplastic problem for a cracked cylinder, Lavit and Tolokonnikov [13] employed a new numerical method [14], which used the Barenblatt model instead of the Griffith crack model [15]. This model contains no singularities of the stress and strain fields at the crack tip, which ensures the validity of the method of elastic solutions [16] — an iterative method for the solution of the elastoplastic problem. This method, however, also has a drawback — the condition that the length of the cohesive zone should be equal to the length of the finite element adjacent to the crack tip. The mesh cannot be refined without decreasing the length of the cohesive zone, which, as in the previous case, casts the correctness of the method. In the solutions given below, the singularities of the stress and strain fields are eliminated in each iteration of the solution of the elastoplastic problem using the finite-element method developed in [17, 18]. In this case, the sizes of the elements and the length of the cohesive zone are independent of each other. The results are compared, where possible, with available data.

1. Formulation and Solution of the Thermoelastoplastic Problem. The thermoelastoplastic deformation of material is described by the constitutive relations

$$\varepsilon_{mn} = \frac{1}{2}\Big(\frac{\partial u_n}{\partial x_m} + \frac{\partial u_m}{\partial x_n}\Big), \qquad \varepsilon_{mn} = \varepsilon^e_{mn} + \varepsilon^p_{mn}, \qquad \varepsilon = \frac{\varepsilon_{mm}}{3},$$
$$\Delta T = T - T_0, \qquad \sigma_{mn} = 3K(\varepsilon - \alpha\Delta T)\delta_{mn} + 2G(\varepsilon^e_{mn} - \varepsilon\delta_{mn}), \tag{1.1}$$
$$\sigma = \sigma_{mm}/3, \qquad d\varepsilon^p_{mn} = d\lambda(\sigma_{mn} - \sigma\delta_{mn}),$$

where x_m are Cartesian coordinates, u_m is the displacement vector, ε_{mn} is the strain tensor, ε^e_{mn} and ε^p_{mn} are the elastic and plastic strain tensors, respectively, T is the temperature, T_0 is the initial temperature, ΔT is the temperature increment, σ_{mn} is the stress tensor, K and G are the elastic moduli, α is the linear-expansion coefficient, δ_{mn} is the Kronecker delta, ε and σ are the average strain and stress, respectively, and $d\lambda$ is an undetermined coefficient. For active loading, the Mises yield condition is satisfied:

$$(\sigma_{mn} - \sigma\delta_{mn})(\sigma_{mn} - \sigma\delta_{mn}) = 2\sigma_Y^2/3. \tag{1.2}$$

In this case, $d\lambda \geqslant 0$ (the equality to zero corresponds to the case of neutral loading). For purely elastic deformation and unloading, the left side of expression (1.2) is smaller than the right side, and, in this case, $d\lambda = 0$.

The solution of the variational equation

$$\int\limits_S \sigma_{mn}\,\delta\varepsilon_{mn}\,dS = \int\limits_l p_k\,\delta u_k\,dl \tag{1.3}$$

(S is the cross-sectional area of the cylinder, l is its boundary contour, and p_k is the load vector applied to the contour), together with the kinematic boundary conditions (in the problem in question, they are reduced to eliminating rigid displacements of the cylinder) and relations (1.1) and (1.2) at a given temperature field, allows to determine all parameters of stress–strain state. The problem is nonlinear, and its solution is found by the iterative method of elastic solutions [16], which was modified for fracture mechanics problem in [19]. The stresses are written as

$$\sigma_{mn} = t_{mn} - 3K\alpha\,\Delta T\,\delta_{mn} + s_{mn},$$

where the stress tensor t_{mn} is related to the strain tensor by Hooke law and the initial stress tensor s_{mn} is proportional to the plastic strain tensor:

$$t_{mn} = 3K\varepsilon\delta_{mn} + 2G(\varepsilon_{mn} - \varepsilon\delta_{mn}), \qquad s_{mn} = -2G\varepsilon^p_{mn}. \tag{1.4}$$

The variational equation (1.3) becomes

$$\int\limits_S t_{mn}\,\delta\varepsilon_{mn}\,dS = \int\limits_l p_k\,\delta u_k\,dl + \int\limits_S (3K\alpha\,\Delta T\,\delta_{ij} - s_{ij})\delta\varepsilon_{ij}\,dS. \tag{1.5}$$

For known initial stresses, Eq. (1.5) is the variational equation of the elastic problem for a cylinder subjected to surface loads (the first term on the right side) and volume loads (the second term). The dependences of the pressure and the temperature field on a certain monotonic loading parameter τ are assumed to be known. The range of τ is divided into M segments, which will be called loading steps. Let the initial stresses s^*_{mn} distributed in the cylinder by the beginning of the next loading step be known. Due to variation in the pressure and (or) the temperature field in the loading step considered, the initial stresses gain increments Δs_{mn}. Assuming that these increments are small, we can use them to approximately replace the differentials ds_{mn}. From relations (1.4) and (1.1), we obtain

$$\Delta s_{mn} = -\Delta\varkappa(t_{mn} - t\delta_{mn} + s^*_{mn}), \qquad \Delta\varkappa = \frac{2G\,\Delta\lambda}{1 + 2G\Delta\lambda}, \quad \Delta\varkappa \in [0;1), \quad t = \frac{t_{mm}}{3} \tag{1.6}$$

(the quantity $d\lambda$ is replaced by $\Delta\lambda$). To determine Δs_{mn} for known values of t_{mn} and s^*_{mn}, it is necessary to know the value of the coefficient $\Delta\varkappa$, which is found from condition (1.2):

$$\Delta\varkappa = 1 - \sigma_Y/\sqrt{1.5(t_{mn} - t\delta_{mn} + s^*_{mn})(t_{mn} - t\delta_{mn} + s^*_{mn})}\,. \tag{1.7}$$

If the calculations using formula (1.7) yield $\Delta\varkappa < 0$, then equality (1.2) is not valid, i.e., purely elastic deformation or unloading takes place. In this case, all relations given above remain valid, but, in them, it is necessary to set $\Delta\varkappa = 0$. The iterative process of elastic solutions is performed as follows. As a first approximation, the initial-stress increments Δs_{mn} are set equal to zero. In this case, the initial stress field $s_{mn} = s^*_{mn}$ is obviously known. Equation (1.5) defining the linear elasticity problem is solved. As a result, the tensor field t_{mn} is found. Next, formulas (1.6) and (1.7) are used to determine the initial-stress increments and then the corrected values of the initial stresses $s_{mn} = s^*_{mn} + \Delta s_{mn}$, after which Eq. (1.5) is solved again, and so long until the iterative process converges, after which the following loading step is made. We note that the condition of smallness of the increments Δs_{mn}, leading to the requirement $\Delta\varkappa \ll 1$, is a necessary condition for the validity of the solution; therefore, the method of elastic solutions can be considered as a correct method for the solution of elastoplastic problems only in the case of no singularities of the stress field.

2. Solution of the Boundary-Value Elastic Problem. Thus, in each iteration of the solution of the elastoplastic problem, it is necessary to solve the elastic problem with specified surface and volume loads. Because, this is a linear fracture mechanics problem, it must be formulated so as to eliminate singularities of the stress field. This is reached by taking into account cohesive forces [15] that attract the opposite crack faces to each other. However, this is not merely a mathematical device. In the neighborhood of the crack tip, there is a narrow zone of large plastic strains, whose propagation during crack growth is primarily responsible for the resistance to this growth. The action of this zone on the remaining material is modeled by cohesive forces [20, 21].

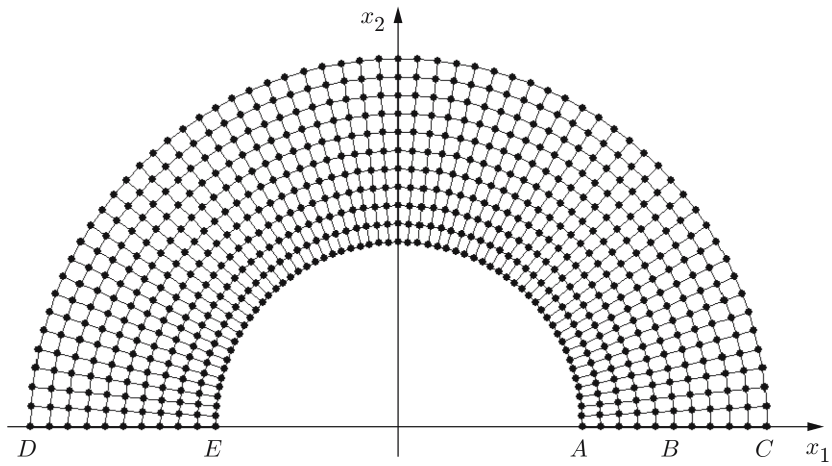

Fig. 2

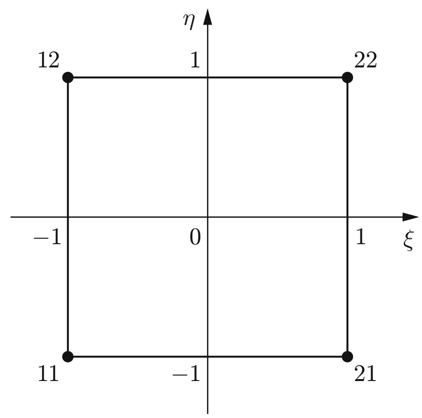

Fig. 3

Fig. 2. Finite-element mesh.

Fig. 3. Finite element in local coordinates.

Because the problem is symmetric, it is sufficient to consider half of the cross section of the cylinder (Fig. 2). The boundary conditions are formulated as follows. The segment of the boundary contour CD (the outer surface of the cylinder) is free of load; on the segments DE and BC, the displacement u_2 and stress σ_{12} are equal to zero (symmetry conditions); the segment EA (the inner surface of the cylinder) is subjected to pressure p; the segment AB (crack surface) is subjected to pressure p, and part of this segment adjacent to the crack tip (point B) is acted upon by cohesive forces. The rigid displacement along the abscissas is subject to the constraint $u_1 = 0$ at the point B.

The elastic problem is solved by the finite-element method [22]. The typical discretization of the computational domain into elements is presented in Fig. 2. In this work, we used square isoparametric elements of the first order (Fig. 3) [22]. The nodes of the elements have double numbering. The global Cartesian coordinates of the points of the element are defined by the formula

$$x_m = L_i(\xi) L_j(\eta) X_m^{ij}, \qquad i, j = 1, 2, \qquad \xi, \eta \in [-1; 1],$$

where X_m^{ij} are the specified global Cartesian coordinates of the nodes (the superscripts denote the node number in the local numbering) and $L_i(\xi)$ are the Lagrangian polynomials

$$L_1(\xi) = (1 - \xi)/2, \qquad L_2(\xi) = (1 + \xi)/2.$$

Let r and θ be polar coordinates and r be reckoned from the crack tip. As $r \to 0$, the stress, strain, and displacements are defined by the asymptotic formulas [11]

$$\sigma_{mn} = K_{\mathrm{I}} \sigma^*_{mn}, \qquad \varepsilon_{mn} = K_{\mathrm{I}} \varepsilon^*_{mn}, \qquad u_m = K_{\mathrm{I}} u^*_m,$$

where K_{I} is the stress intensity factor (in this case, because of the symmetry of the problem, $K_{\mathrm{II}} = 0$); σ^*_{mn}, ε^*_{mn}, and u^*_m are known functions of the coordinates [11]. In particular, in the case of plane deformation

$$u_1^* = \frac{2(1+\nu)}{E} \sqrt{\frac{r}{2\pi}} \cos\frac{\theta}{2}\Big(1 - 2\nu + \sin^2\frac{\theta}{2}\Big), \qquad u_2^* = \frac{2(1+\nu)}{E} \sqrt{\frac{r}{2\pi}} \cos\frac{\theta}{2}\Big(2(1 - \nu) - \cos^2\frac{\theta}{2}\Big)$$

(E is Young's modulus and ν is Poisson's constant).

The displacements inside any finite element are specified as

$$u_m = L_i(\xi) L_j(\eta) U_m^{ij} + K_{\mathrm{I}} u^*_m, \tag{2.1}$$

where U_m^{ij} are nodal displacements [displacements of the nodes ignoring the contribution of the second term in formulas (2.1)]. The stress intensity factor K_{I} is unknown and, along with the nodal displacements, is a varied parameter. Specification of the displacement field in the form of (2.1) provides, first, a correct asymptotic representation of the stresses and strains with approach to the crack tip and, second, continuity of the displacement field on the boundaries of the elements.

Next, we employ the standard finite-element procedure to reduce the solution of the problem to the solution of a system of linear algebraic equations [22]. The basic variational equation (1.5) written for one term becomes

$$\begin{gathered}\{a_0[(1-\nu)a_{ijmn}+(1-2\nu)b_{ijmn}/2]U_1^{mn}+a_0[\nu c_{ijmn}+(1-2\nu)c_{mnij}/2]U_2^{mn}\\ +(d_{ij11}+e_{ij12})K_{\mathrm{I}}\}\delta U_1^{ij}+\{a_0[\nu c_{mnij}+(1-2\nu)c_{ijmn}/2]U_1^{mn}\\ +a_0[(1-\nu)b_{ijmn}+(1-2\nu)a_{ijmn}/2]U_2^{mn}+(e_{ij22}+d_{ij12})K_{\mathrm{I}}\}\delta U_2^{ij}\\ +\{a_0[(1-\nu)f_{mn11}+\nu f_{mn22}+(1-2\nu)g_{mn12}]U_1^{mn}+a_0[(1-\nu)g_{mn22}+\nu g_{mn11}\\ +(1-2\nu)f_{mn12}]U_2^{mn}+hK_{\mathrm{I}}\}\delta K_{\mathrm{I}}=\chi_{ij}\,\delta U_1^{ij}+\psi_{ij}\,\delta U_2^{ij}+\omega\,\delta K_{\mathrm{I}},\end{gathered} \tag{2.2}$$

where the coefficients are defined by the formulas

$$\begin{gathered}a_0=\frac{E}{(1-2\nu)(1+\nu)},\qquad a_{ijmn}=\int\limits_S\Phi_{ij}\Phi_{mn}\,dS,\qquad b_{ijmn}=\int\limits_S F_{ij}F_{mn}\,dS,\\ c_{ijmn}=\int\limits_S\Phi_{ij}F_{mn}\,dS,\qquad d_{ijmn}=\int\limits_S\Phi_{ij}\sigma^*_{mn}\,dS,\qquad e_{ijmn}=\int\limits_S F_{ij}\sigma^*_{mn}\,dS,\\ f_{ijmn}=\int\limits_S\Phi_{ij}\varepsilon^*_{mn}\,dS,\qquad g_{ijmn}=\int\limits_S F_{ij}\varepsilon^*_{mn}\,dS,\qquad h=\int\limits_S\sigma^*_{mn}\varepsilon^*_{mn}\,dS,\\ \chi_{ij}=\int\limits_l p_1L_i(\xi)L_j(\eta)\,dl-\int\limits_S[(3K\alpha\Delta T+s_{11})\Phi_{ij}+s_{12}F_{ij}]\,dS,\\ \psi_{ij}=\int\limits_l p_2L_i(\xi)L_j(\eta)\,dl-\int\limits_S[s_{12}\Phi_{ij}+(3K\alpha\Delta T+s_{22})F_{ij}]\,dS,\\ \omega=\int\limits_l p_mu^*_m\,dl-\int\limits_S(3K\alpha\,\Delta T\,\delta_{mn}+s_{mn})\varepsilon^*_{mn}\,dS.\end{gathered} \tag{2.3}$$

The contour integrals in formulas (2.3) are different from zero only for elements whose sides are subjected to external loading. The functions in the integrands for coefficients (2.3) are found from the expressions

$$\begin{gathered}\Phi_{ij}(\xi,\eta)=[(-1)^iL_j(\eta)\,\partial_1\xi+(-1)^jL_i(\xi)\partial_1\eta]/2,\\ F_{ij}(\xi,\eta)=[(-1)^iL_j(\eta)\,\partial_2\xi+(-1)^jL_i(\xi)\,\partial_2\eta]/2,\\ \partial_m=\frac{\partial}{\partial x_m},\qquad\begin{pmatrix}\partial_1\xi & \partial_2\xi\\ \partial_1\eta & \partial_2\eta\end{pmatrix}=\begin{pmatrix}\partial_\xi x_1 & \partial_\eta x_1\\ \partial_\xi x_2 & \partial_\eta x_2\end{pmatrix}^{-1},\\ \partial_\xi x_m=(-1)^iL_j(\eta)X_m^{ij}/2,\qquad\partial_\eta x_m=(-1)^jL_i(\xi)X_m^{ij}/2.\end{gathered}$$

Summation of expressions (2.2) over all finite elements with Conversion from the two-dimensional to one-dimensional numbering of unknowns and taking into account that one node is contained in several elements leads to the system of $N+1$ linear algebraic equations

$$TZ=P, \tag{2.4}$$

where the first N elements of the column matrix Z are the required nodal displacements and $z_{N+1}=K_{\mathrm{I}}$. Displacements of the nodes lying on the boundary contour segments BC and DE (see Fig. 2) should satisfy the kinematic boundary conditions. Because the displacements u_2^* are equal to zero on the segment BC, the conditions are taken into account using the standard method [22]: the corresponding elements of the vector of the right sides P and the corresponding rows and columns of the matrix T, except for diagonal terms are set equal to zero. On the segment DE, the displacements u_2^* are different from zero. In this case, the kinematic boundary conditions are satisfied as follows. Let j be the number of a nodal displacement such that its sum with the displacement $K_{\rm I} u_2^*$ which, at the point considered, is equal, for example, to $bK_{\rm I}$, should be zero. In this case, because $\delta z_j = -b\,\delta K_{\rm I}$, the jth row of the matrix T multiplied by $-b$ needs to be added to the $(N+1)$th row, and then the jth column multiplied by $-b$ needs to be added to the $(N+1)$th column. Next, according to the standard approach [22], in the jth row and the jth column, all elements are set equal to zero, except for the diagonal element, which is set equal to unity, and except for the element $t_{j,N+1}$, which is set equal to b.

The matrix T (converted according to the boundary conditions) is not a band matrix; therefore, to solve system (2.4), it is reasonable to split it into the system of the first N equations, whose coefficient matrix is a band matrix, and the $(N+1)$th equation. Let the vector of the unknowns Y include the first N components of the vector Z, the vector of the right sides B include the first N components of the vector P, and the matrix A include the first N rows and N columns of the matrix T. System (2.4) is equivalent to the system

$$\begin{gathered} AY = B - CK_{\rm I}, \\ \sum_{i=1}^{N} t_{N+1,i} y_i + t_{N+1,N+1} K_{\rm I} = p_{N+1}, \end{gathered} \tag{2.5}$$

where the vector C consists of the first N elements of the $(N+1)$th column of the matrix T. The matrix A is apparently a band one. Solving the first (matrix) equation of system (2.5) first with the right side B, and then with the right side $-C$, we obtain a solution of the form

$$Y = Y_1 + K_{\rm I} Y_2.$$

Next, from the second equation of system (2.5), it is easy to determine the value of $K_{\rm I}$.

Cohesive forces are applied to the boundary segment AB in a direction opposite to the ordinate direction. The modulus of these forces varies along the abscissa as [19]

$$q(x_1) = \begin{cases} q_*(1 - 3\zeta^2 + 2\zeta^3), & \zeta \in [0,1], \\ 0, & \zeta > 1, \end{cases}$$

where $\zeta = (R_1 + a - x_1)/\delta$ ($\delta \ll a$ is the length of the cohesive zone). For the specified value of δ, the cohesive forces are defined by their maximum value q_*, which is found from the condition of no singularity of the stress field at the crack tip. Because of the linearity of the elastic problem, the stress intensity factor can be represented as the sum

$$K_{\rm I} = K_{\rm I1} + q_* K_{\rm I2}$$

($K_{\rm I1}$ is the intensity factor for stresses that arise under the action of pressure, temperature gradient, and initial stresses and $K_{\rm I2}$ is the intensity factor for stresses that arise under the action of cohesive forces at $q_* = 1$). Setting $K_{\rm I} = 0$, we find the value of q_* and, as a consequence, the total stress field that has no singularity.

The energy characteristic of fracture (the J-integral) is expressed in terms of the cohesive forces by the Rice formula [11]

$$J = -2 \int\limits_{R_1+a-\delta}^{R_1+a} q \frac{\partial u_2}{\partial x_1}\, dx_1.$$

This formula is also valid in the cases where the value of J ignoring cohesive forces cannot be found as a path independent contour integral, for example, under the action of a nonuniform temperature field [21].

3. Calculation Results. The method proposed here was used to solve a number of thermoelastoplastic problems for a cracked cylinder. In all calculation examples given below, the finite-element mesh was refined as long as the first three significant figures of the result (the values of the J-integral) changed. In the final version, the number of equations in the system was 60,702. We first solved the problem of elastoplastic deformation of a cylinder

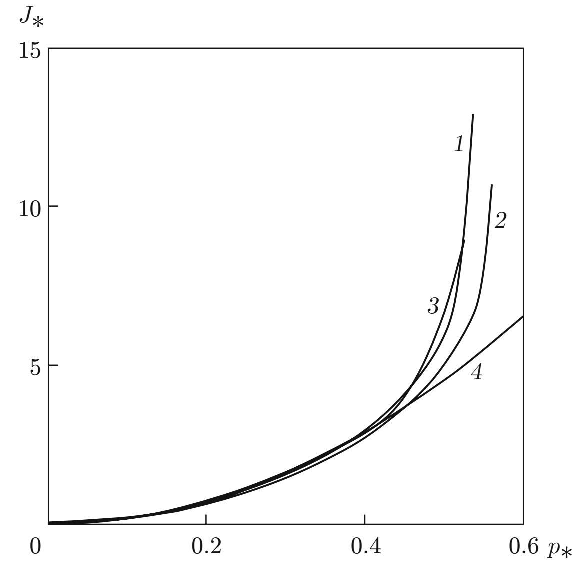

Fig. 4

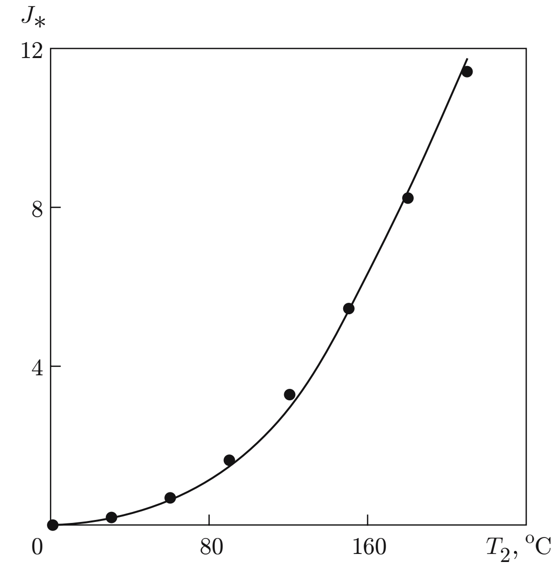

Fig. 5

Fig. 4. J-integral versus pressure in the case of an unheated cylinder: curves 1–3 refer to the calculation taking into account elastoplastic deformation for $\delta/a = 0.05$ (1) and 0.1 (2); curve 3 is the calculation result of [8]; curve 4 refers to the calculation taking into account only elastic deformation [3].

Fig. 5. J-integral versus temperature on the outer surface of the cylinder: the curve is the result of calculation using the method developed; the points are the calculation results of [9].

subjected to internal pressure, whose results can be compared with the data of [8]. The calculations were performed for the following initial data: Young's modulus $E = 2.15 \cdot 10^5$ N/mm^2, Poisson's constant $\nu = 0.3$, yield point $\sigma_Y = 275$ N/mm^2, wall-thickness parameter $\beta = R_2/R_1 = 2$, and relative crack length $a_* = a/(R_2 - R_1) = 0.5$. Figure 4 shows the calculated curve of the J-integral versus pressure in the cylinder channel in dimensionless variables:

$$p_* = \frac{p}{p_f}, \qquad p_f = \frac{2\sigma_Y}{\sqrt{3}} \ln\beta, \qquad J_* = \frac{EJ}{a\sigma_Y^2} \tag{3.1}$$

(p_f is the limiting internal pressure for the cylinder without a crack [23]).

Curves 1–3 are calculated taking into account elastoplastic deformation before the attainment of the ultimate pressure (the pressure at which the cylinder lost the load-carrying ability). In Fig. 4, it is evident that the length of the cohesive zone has a weak effect on the calculation results: as it changes by a factor of two, the limiting pressure changes by only 4.2%. The results of calculations using the method developed agree with the results obtained in [8]. In the problem considered, accounting for the possibility of plastic deformation leads to relations that differ significantly from the results taking into account only elastic deformation (curve 4).

Figure 5 shows the results of solution of the thermoelastoplastic problem for a cylinder heated from the outer surface at $p = 0$ and the following initial data: $E = 2 \cdot 10^5$ N/mm^2, $\nu = 0.3$, $\sigma_Y = 200$ N/mm^2, $\beta = 1.2$, $a_* = 0.5$, $\alpha = 10^{-5}$ 1/°C. The steady-state temperature field in the cylinder is defined by the formula

$$T = T_2 + (T_1 - T_2) \ln(r/R_2)/\ln(R_1/R_2), \tag{3.2}$$

where T_1 and T_2 are the temperatures of the inner and outer surfaces of the cylinder, respectively, and r is the radial coordinate. The calculations were performed for $T_0 = T_1 = 0$°C and $\delta/a = 0.05$. A comparison of the calculation results with the data of [9] obtained by another method show that they are in good agreement (Fig. 5).

The case of the joint action of pressure and a temperature field is more difficult to calculate and more important for engineering practice. In the case of considerable heating, it is necessary to take into account the temperature dependence of the yield point, which is represented as $\sigma_Y = \sigma_{Y0}\psi(T)$, where $\psi(T)$ is a dimensionless function and σ_{Y0} is the yield point at $\psi = 1$. The values of the function $\psi(T)$ for high-strength steels are listed

TABLE 1

T, °C	$\psi(T)$	T, °C	$\psi(T)$
0	1,00	500	0.57
100	1.00	600	0.35
200	1.00	700	0.19
300	0.97	800	0.09
400	0.83		

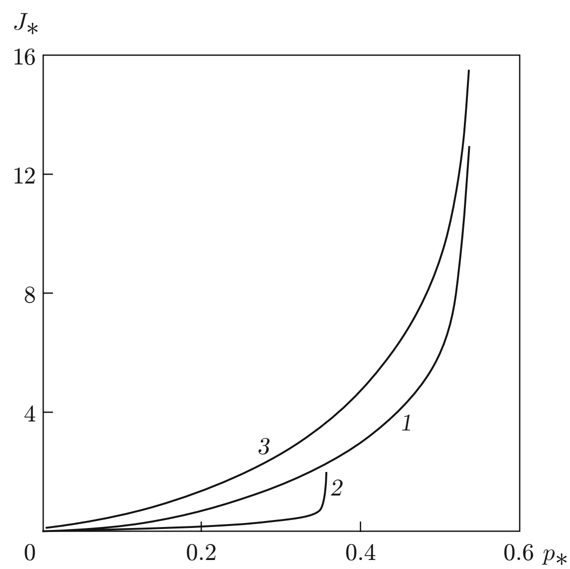

Fig. 6. J-integral versus pressure in the cylinder channel under different loading conditions: 1) unheated cylinder; 2) the joint action of heating and pressure; 3) heating of the cylinder with subsequent cooling and pressure loading.

in Table 1. The calculations were performed for the following initial data: $E = 2.15 \cdot 10^5$ N/mm^2, $\nu = 0.3$, $\sigma_{Y0} = 275$ N/mm^2, $\beta = 2$, $a_* = 0.5$, $\delta/a = 0.05$, $\alpha = 10^{-5}$ 1/°C, and $T_0 = 20$°C. The calculation results are given in Fig. 6 [the quantities p_* and J_* are defined by formulas (3.1), in which by the quantity σ_Y is meant the quantity σ_{Y0}]. The difference between the curves is due to differences in loading conditions. Curve 1 in Fig. 6 (curve 1 in Fig. 4) characterizes the resistance of the unheated cylinder. Curve 2 is obtained for the steady-state temperature distribution (3.2), and the temperature of the inner and outer surfaces increase in proportion to the pressure as follows:

$$T_1 = T_0 + 1460 p_*, \qquad T_2 = T_0 + 1060 p_*.$$

Curve 3 corresponds to the following loading conditions: the cylinder is first heated at $p = 0$ to temperatures $T_1 = 750$°C and $T_2 = 550$°C [the temperature distribution over the cross section of the cylinder is given by formula (3.2)], and the cylinder is then cooled to temperature T_0, after which its inner surface is subjected to pressure loading. The action of the residual stress field formed after heating with subsequent cooling is similar to the action of the stress field due to the action of pressure, as a result of which curve 3 is above curve 1.

If the strength of the cylinder is estimated from its load-carrying ability, the determining loading regime is the one described by curve 2 in Fig. 6, but if fatigue failure is possible or the critical value of the J-integral is small enough, the loading regime described by curve 3 is the determining one. Thus, the loading regime can influence the estimation of the strength of the cylinder.

This work was supported by the Russian Foundation for Basic Research (Grant Nos. 04-01-00247 and 07-01-96402).

REFERENCES

1. O. L. Bowie and C. E. Freese, "Elastic analysis for a radial crack in a circular ring," *Eng. Fract. Mech.*, **4**, 315–321 (1972).
2. R. W. E. Shannon, "Stress intensity factors for thick-walled cylinders," *Int. J. Pressure Vessels Piping*, **2**, 19–29 (1974).
3. C. P. Andrasic and A. P. Parker, "Stress intensity factors for externally and internally cracked pressurized thick cylinders with residual and thermal stresses," in: *Fracture Mechanics Technology Applied to Material Evaluation and Structure Design*, Proc. Int. Conf. (Melbourne, Australia, August 10–13, 1982), The Hague (1983), pp. 193–214.
4. C. P. Andrasic and A. P. Parker, "Dimensionless stress intensity factors for cracked thick cylinders under polynomial crack face loadings," *Eng. Fract. Mech.*, **19**, No. 1, 187–193 (1984).
5. A. P. Parker, J. H. Underwood, J. E. Throop, and C. P. Andrasic, "Stress intensity and fatigue crack growth in a pressurized, autofrettaged thick cylinder," *ASTM Spec. Tech. Publ.*, No. 791, I-216–I-237 (1983).
6. S. L. Pu and M. A. Hussain, "Stress-intensity factors for radial cracks in a partially autofrettaged thick-wall cylinder," *ASTM Spec. Tech. Publ.*, No. 791, I-194–I-215 (1983).
7. J. D. G. Sumpter, Elastic–plastic fracture analysis and design using the finite element method: PhD thesis, Imperial College, London (1973).
8. C. L. Tan and K. H.Lee, "Elastic–plastic stress analysis of a cracked thick-walled cylinder," *J. Strain Anal.*, **18**, 253–260 (1983).
9. J. L. Cheissoux, "Numerical applications of path independent integrals in the case of thermal strains, creep analysis and mixed mode situations," in: *Advances in Fracture Research* (Proc. of the 6th Int. Conf. Fract., 1984), Vol. 5, Pergamon Press, Oxford–New York (1986), pp. 3623–3630.
10. W. Zhigun, "Elastic–plastic fracture analysis of a thick-walled cylinder," *Int. J. Pressure Vessels Piping*, **63**, 165–168 (1995).
11. J. R. Rice, "Mathematical analysis in the fracture mechanics," in: H. Liebowitz (ed.), *Fracture*, Vol. II, Academic Press, New York (1968).
12. L. H. Larsson, "A calculational round robin in elastic–plastic fracture mechanics," *Int. J. Pressure Vessels Piping*, **11**, 207–228 (1983).
13. I. M. Lavit and L. A. Tolokonnikov, "Thermoelastoplastic fracture mechanics problem for a cylinder with internal cracks," in: *Applied Problems of Strength and Plasticity. Methods of Solution* [in Russian], Izd. Gor'k. Gos. Univ., Gor'kii (1990), pp. 55–60.
14. I. M. Lavit, "Steady growth of a crack in an elastoplastic material," *Probl. Prochn.*, No. 7, 18–23 (1988).
15. G. I. Barenblatt, "Mathematical theory of equilibrium brittle-fracture cracks," *Zh. Prkl. Mekh. Tekh. Fiz.*, No. 4, 3–56 (1961).
16. A. A. Il'yushin, *Plasticity*, Part 1: *Elastoplastic Deformation* [in Russian], Gostekhteoretizdat, Moscow–Leningrad (1948).
17. N. V. Krukova and I. M. Lavit, "The finite-element method in linear fracture mechanics problems," in: *Proc. of the 3rd Europ. Conf. on Comput. Mech.* (Lisbon, June 5–8, 2006), ECCM, Lisbon (2006). CD-ROM.
18. I. M. Lavit and N. V. Sibirtseva, "Finite-element method for solving linear fracture mechanics problem," *Izv. Tul'sk. Gos. Univ., Aktual. Probl. Mekh.*, No. 2, 96–102 (2006).
19. I. M. Lavit, "Crack growth in quasibrittle fracture under monotonically increasing and cyclic loads," *Izv. Ross. Akad. Nauk, Mekh. Tverd. Tela*, No. 2, 109–120 (2001).
20. G. I. Barenblatt, "Some general concepts of the mathematical theory of brittle fracture," *Prikl. Mat. Mekh.*, **28**, No. 4, 630–643 (1964).
21. I. M. Lavit, "Energy balance in the neighborhood of the crack tip in an elastoplastic medium," *Izv. Ross. Akad. Nauk, Mekh. Tverd. Tela*, No. 3, 123–131 (2001).
22. O. C. Zienkiewicz, *The Finite Element Method in Engineering Science*, McGraw-Hill, London (1977).
23. L. M. Kachanov, *Foundations of the Theory of Plasticity*, North-Holland, Amsterdam–London (1971).